

Metals and Ceramics Division

**Cavitation as a Mechanism to Enhance Wetting in a Mercury Thermal Convection Loop**

S. J. Pawel\*  
E. T. Manneschildt\*  
R. P. Taleyarkhan†  
S. H. Kim†  
J. R. DiStefano\*

\*Metals and Ceramics Division  
†Engineering Technology Division

Date Published: May 2001

Prepared for the  
U.S. Department of Energy  
Spallation Neutron Source

Prepared by the  
OAK RIDGE NATIONAL LABORATORY  
Oak Ridge, Tennessee 37831-6285  
Operated by  
UT-Battelle, LLC  
For the  
U.S. DEPARTMENT OF ENERGY  
Under contract DE-AC05-00OR22725



## CONTENTS

	<b>Page</b>
FIGURES .....	v
ABSTRACT .....	vii
1. INTRODUCTION .....	1
2. PROOF-OF-CONCEPT EXPERIMENTS .....	5
3. MODIFIED TCL EXPERIMENTS .....	15
4. CONCLUSIONS .....	21
ACKNOWLEDGEMENTS .....	23
REFERENCES .....	25



## FIGURES

Figure	Page
<p><b>1 Schematic arrangement of the bench-top cavitation experiments.</b>                      The type 316L stainless steel coupon was immersed in mercury at room temperature and pressure waves were generated with the acoustic driver .....</p>	6
<p><b>2 Photomicrographs of the as-polished cross section of an unexposed coupon (a,b,c) and a coupon exposed to cavitation conditions in room temperature mercury (d,e,f).</b> The unexposed coupon (photos in left column) exhibits less surface roughness than the exposed coupon (compare equivalent magnification photos for exposed/unexposed conditions) .....</p>	8
<p><b>3 Scanning electron microscope images of the surface of a virgin 316L coupon.</b> The lapping marks and debris are typical of an as-machined stainless steel surface .....</p>	9
<p><b>4 Representative profile analysis for the virgin coupon surface.</b> Relative elevation along the trace (white line in photo) is given by the graph at the bottom. In this case, the elevation difference between the high point and low point (large dots on trace) is about 1 <math>\mu\text{m}</math>. Except for isolated areas (from which inclusions have been pulled to create a pit-like region), the bulk surface is smooth with nominal surface relief approximately 0.5<math>\mu\text{m}</math> .....</p>	10
<p><b>5 Scanning electron microscope images of the surface of the 316L coupon exposed to cavitation conditions in mercury.</b> Compared to the virgin coupon shown in Fig. 3, the surface here is rough and irregular .....</p>	11
<p><b>6 Representative profile analysis for a 316L coupon exposed to cavitation conditions in the bench-top experiment.</b> Relative elevation along the trace (white line in photo) is given by the graph at the bottom. In this representative case, the elevation difference between the high point and low point (large dots on trace) is almost 15 <math>\mu\text{m}</math>. Even deeper “pits” are evident in this area .....</p>	12
<p><b>7 Schematic diagram of TCL modified by the addition of an ultrasonic transducer.</b> Overall, the actual loop is about 1 m in height and about half that wide. The tubing is 316L stainless steel of 2.5 cm diameter .....</p>	16



## **ABSTRACT**

Type 316L stainless steel was statically tested under cavitation conditions via an ultrasonic transducer externally mounted on a tube filled with ambient mercury. During the preliminary exposure (24 h, 20 kHz, 1.5 MPa), cavitation resulted in apparent wetting of the specimens by mercury as well as general surface roughening and wastage similar to erosion damage. Subsequently, a thermal convection loop identical to those used previously to study thermal gradient mass transfer was modified to include an externally-mounted donut-shaped transducer in order to similarly produce cavitation and wetting at temperatures prototypic of those expected in the SNS target. However, a series of attempts to develop cavitation and wetting on 316L specimens in the thermal convection loop was unsuccessful.





## 1. INTRODUCTION

The Spallation Neutron Source (SNS) will generate neutrons via interaction of a 1.0 GeV proton beam with a liquid mercury target. Type 316L/316LN austenitic stainless steel has been selected as the primary target containment material<sup>1</sup> based on a favorable combination of several factors, including resistance to corrosion by mercury, well-characterized behavior in a radiation environment, and the absence of a significant ductile-brittle transition temperature such as that found in irradiated ferritic stainless steels.

The energy deposited in the mercury target by the pulsed proton beam (beam power absorbed in the target will be about 1.2 MW on a time-averaged basis) will be removed by circulating the mercury through standard heat exchangers. Various fluid dynamics computations and simulations of conditions expected in the target predict maximum bulk mercury temperatures on the order of 150°C with nominal temperatures closer to 100-120°C. The mercury temperature at the target inlet is expected to be near ambient temperature.

As a result of the temperature gradient in flowing mercury, one of the potential compatibility problems under investigation in support of the SNS Project is thermal gradient mass transfer. In this form of corrosion, dissolution of the container material by the liquid in relatively high temperature (high solubility) regions is accompanied by deposition of excess solute in relatively colder regions.<sup>2</sup> As a result, corrosion of the high temperature region is not limited by solubility considerations and thus can be accelerated over what would be experienced in an isothermal/stagnant system. In addition, in the cold regions, deposition of solute material has been known to cause flow disruptions and can even plug flow paths in liquid metal loops.<sup>3</sup> Among the major alloying elements of stainless steels, nickel is expected to have the highest solubility in mercury<sup>4</sup> at SNS operating temperatures, and therefore this element may be the most susceptible to mass transfer.

At the expected SNS operating temperatures, pure mercury does not readily wet 316/316L stainless steel. Without chemical wetting, which can be characterized macroscopically by a low contact angle between a mercury droplet and a surface, any potential corrosion process is inhibited. However, mercury can be made to wet 316/316L in air or vacuum by raising the temperature to 225-275°C.<sup>5</sup> Despite the relatively low expected operating temperatures, chemical wetting of containment surfaces may be encouraged in the SNS target by a combination of several other factors:

1. thermal hot spots,
2. radiation damage in the presence of mercury, and
3. generation of fresh (oxide-free) surfaces that result from potential cavitation and thermal shock/fatigue loading to which the target containment material will be exposed.

The potential for wetting resulting from the above factors makes it desirable for tests of compatibility to develop wetting in order to examine “worst case” interaction between mercury and the target containment. In this vein, a series of compatibility experiments for the SNS target station<sup>6-8</sup> utilized thermal convection loops (TCLs) with relatively high peak temperatures (near 300°C) to encourage wetting. While some degree of wetting and interaction of mercury with the stainless steel coupons was observed in these experiments, overall attack/dissolution was very minor and wetting by mercury was somewhat sporadic and inconsistent in these TCL experiments.

In the SNS, the incident proton beam interacting with the target mercury will be pulsed. The duration of each pulse is short ( $<1\mu\text{s}$ ) and the temperature rise of the affected volume is small (a few °C), but the rate of temperature rise during each pulse is exceptionally high (order of  $10^7\text{°C/s}$ ). The expansion of the affected volume with each pulse gives rise to a thermal-shock induced pressure wave, which travels into the surrounding mercury. When the compression wave

reaches a boundary (e.g., the containment wall), it will be reflected back with a change of phase. The resulting rarefaction wave travels back into/through the mercury, exposing the mercury to transient negative pressures. When the liquid mercury is exposed to sufficient negative pressure, microscopic bubbles are expected to form in the mercury. Previous research<sup>9,10</sup> indicates less than one MPa is required to generate bubbles in nominal purity mercury at SNS temperatures. When the bubbles collapse (in principle, with each pulse cycle) at/near the containment surface, the energy released (typically a “jetting” action of liquid at extreme velocity) effectively erodes the surface through a scrubbing action. This form of mechanical damage, termed cavitation, potentially could be a localized wastage issue for the target containment. In addition, due to the erosive action of the collapsing bubbles, cavitation may be expected to remove the air-formed passive film from the containment surface, thus rendering it more susceptible to chemical wetting by mercury and any subsequent dissolution and mass transfer that ensues.

Calculations<sup>11</sup> for the SNS operating conditions suggest that negative pressures sufficient to induce cavitation will be routinely present in the target near the beam window. Therefore, there is a potential for wetting and interaction between the mercury and stainless steel in the SNS even though it will operate at temperatures well below those used in the prior TCL tests. The experiments reported here represent a laboratory effort to utilize cavitation as a mechanism to induce wetting in TCLs operating at prototypic SNS temperatures. Although there is uncertainty as to whether the frequency and magnitude of pressure oscillations examined here will be prototypic of the dominant modes expected in the SNS, the ultrasonic energy in these tests could at least act as a tool to determine if low temperature wetting can occur.



## 2. PROOF-OF-CONCEPT EXPERIMENTS

Relatively little work has been done to examine cavitation in mercury as a mechanism by which wetting of stainless steel can occur. In one study associated with SNS,<sup>12</sup> polished specimens of stainless steel were attached to the tip of a velocity transformer and ultrasonically agitated at 20 kHz in mercury at various vibrational amplitudes to examine cavitation damage on the surfaces. The authors found apparent wetting (low contact angle, adherent mercury) and relatively significant damage on the stainless steel surfaces measured as wastage of many  $\mu\text{m}/\text{h}$  for up to eight hours in tests with average mercury temperature of 42°C. Frequency and amplitude relevance to SNS aside, however, a subtle but perhaps important difference between these experiments<sup>12</sup> and cavitation in the SNS target containment is that the target surfaces will receive pressure pulses generated at distant locations in the mercury. In the experiments of reference 12, the surfaces themselves created pressure pulses via externally driven vibrational motion. In the present experiments, rather than ejecting energy into the mercury through the test specimen, pressure waves are created by energy deposited in the mercury from vibrations in the container wall, which then interact with the surrounding structures and specimens.

In an initial bench-top experiment, the simple arrangement shown in Fig. 1 was used to examine the feasibility of attaching an ultrasonic transducer to a standard TCL to generate cavitation, and thereby potential wetting, on 316L stainless steel coupons at near prototypic mercury temperatures. The apparatus consisted of a cylindrical glass container filled with pure mercury from the master batch of material used for all of the compatibility experiments to date.<sup>6</sup> A rectangular coupon (2.5 cm x 1.9 cm x 0.1 cm) of mill-annealed and surface-ground 316L stainless steel, identical to those used in many previous experiments,<sup>6,7</sup> was attached to the end of a support rod and positioned in the center of the glass cylinder. A cylindrical ultrasonic transducer was coupled to the outside surface of the glass container and a programmable waveform generator and amplifier were used to drive the transducer. A pill-microphone (and

later a calibrated pressure transducer) was used to monitor changes in the wave shape and as an indicator of the onset of cavitation.

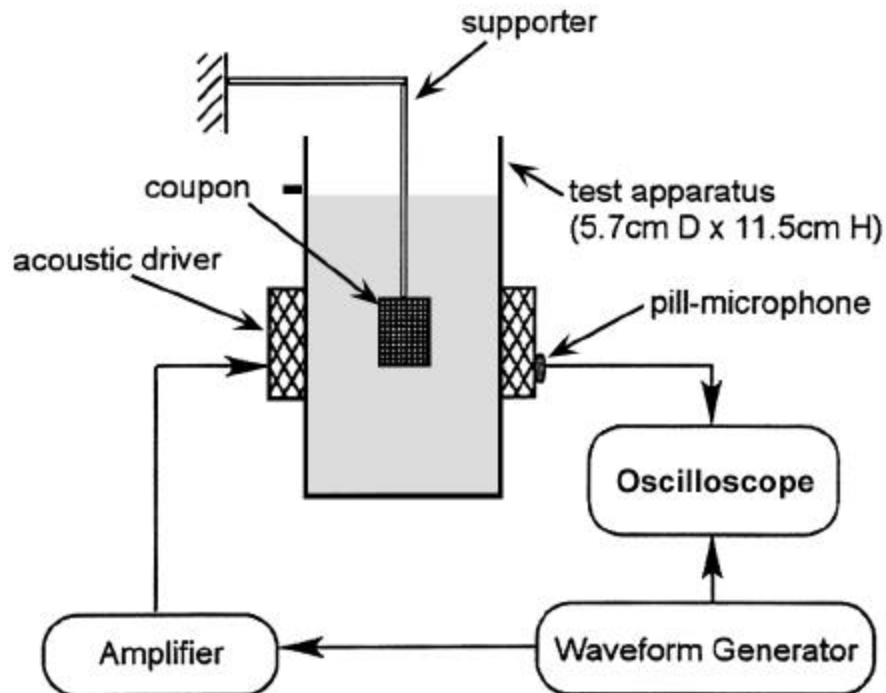


**Fig. 1. Schematic arrangement of the bench-top cavitation experiments.** The type 316L stainless steel coupon was immersed in mercury at room temperature and pressure waves were generated with the acoustic driver.

Initially, specimens were exposed to the mercury for 24 hours at room temperature without power to the transducer. These experiments yielded no change in coupon weight or appearance and no tendency for mercury to cling to the specimen, which would indicate wetting. Subsequently, with the ultrasonic transducer driven at ~20 kHz – the first resonant mode of the system – with peak-to-peak pressure wave oscillation of about 1.5 MPa, cavitation was induced on the specimen surfaces for 24 hours at room temperature. These conditions (20 kHz, 1.5 MPa) are within the realm of possibility for SNS operation. Several different vibrational modes are expected to exist, including one at several tens of kHz corresponding to the interaction of waves

within thin plates or within the narrow mercury volume confined by the plates, which is a planned design feature of the SNS target. Such a high frequency may not be a dominant mode; however, it is expected to exist locally in these regions. When examined immediately after the cavitation exposure, mercury was found to cling to most of the specimen surface. Following light wiping and a brief ultrasonic soak in acetone to remove the residual mercury, the post-test coupon exhibited a significant weight loss (about 10 mg) and a significantly roughened surface. Clearly, the ultrasonic agitation and induced cavitation at the specimen surface encouraged interaction with the mercury.

To quantify the extent of interaction, two comparisons are useful. One is to consider the results from the initial TCL experiment<sup>6</sup> in which wetting and interaction of mercury with mill-annealed and surface-ground 316L was observed. In that TCL test, coupons identical to those exposed in the present experiment were used. At Hg temperatures above about 255°C (the apparent “wetting” temperature) the specimens had developed a thin ferritic surface layer that was porous and substantially leached of nickel and chromium, with the thickness of the surface layer increasing with increasing exposure temperature. The maximum thickness of this layer was observed on the coupon exposed at the top of the TCL hot leg (305°C) for 5000 h; this coupon had a ~10 μm surface layer and exhibited a weight loss of about 16 mg in 5000 h. In the cavitation experiment, the same size coupon was found to lose ~10 mg in only 24 h at room temperature.

It is also useful to compare the surface profiles of 316L specimens before and after exposure to cavitation conditions in mercury. Figure 2 is a montage of photomicrographs showing the as-polished cross section of an unexposed coupon and that of a coupon exposed to mercury under cavitation conditions for 24 h at room temperature. The unexposed coupon exhibited modest surface irregularities with a nominal peak-to-valley surface relief of ~2-3 μm (Fig. 2a,b) and a maximum of about 5 μm (Fig. 2c). In contrast, the specimen exposed to

cavitation conditions had a more irregular surface with typical peak-to-valley distances of ~10-12  $\mu\text{m}$  (Fig. 2d,e) and maximum of about 15  $\mu\text{m}$  (Fig. 2f).

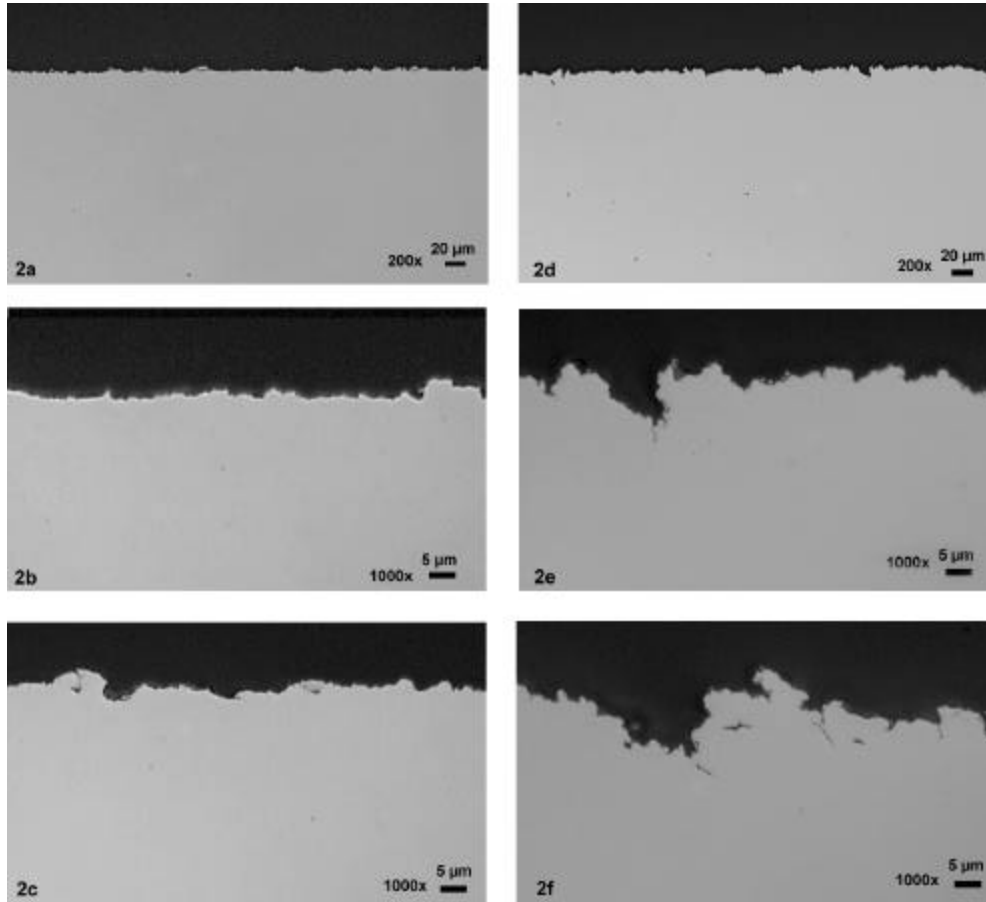


**Fig. 2. Photomicrographs of the as-polished cross section of an unexposed coupon (a,b,c) and a coupon exposed to cavitation conditions in room temperature mercury (d,e,f). The unexposed coupon (photos in left column) exhibits less surface roughness than the exposed coupon (compare equivalent magnification photos for exposed/unexposed conditions).**

The difference in surface profiles between these specimens is similar in magnitude, but more striking in appearance, when viewed with the scanning electron microscope. Figure 3 shows representative backscattered electron images of the surface of an unexposed coupon. The photos show that the surface is largely smooth with occasional lapping marks or locations where an inclusion has been dragged from the surface by the machining operation. Figure 4 gives a stereo image view of the surface along with a profile analysis for a typical area. [The image



software can “merge” photos taken from slightly different angles, say 5°, and calculate surface relief on a very detailed basis (linear spacing of ~0.01 μm for measurement).] As indicated by the photo and profile analysis in Fig. 4, most of the surface is relatively smooth and exhibits only ±0.5 μm or so of surface relief, with small areas of slightly greater relief.

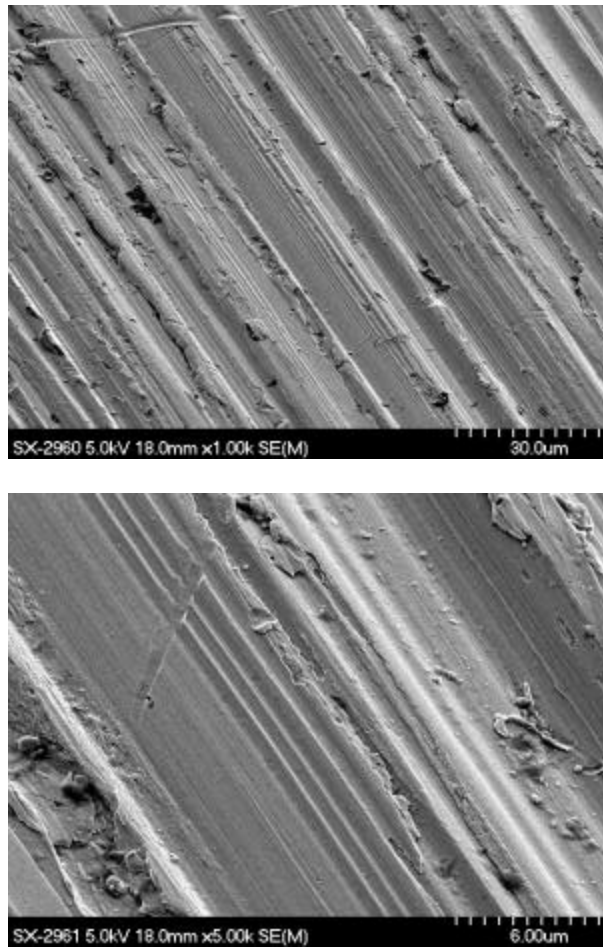


**Fig. 3. Scanning electron microscope images of the surface of a virgin 316L coupon.** The lapping marks and debris are typical of an as-machined stainless steel surface.

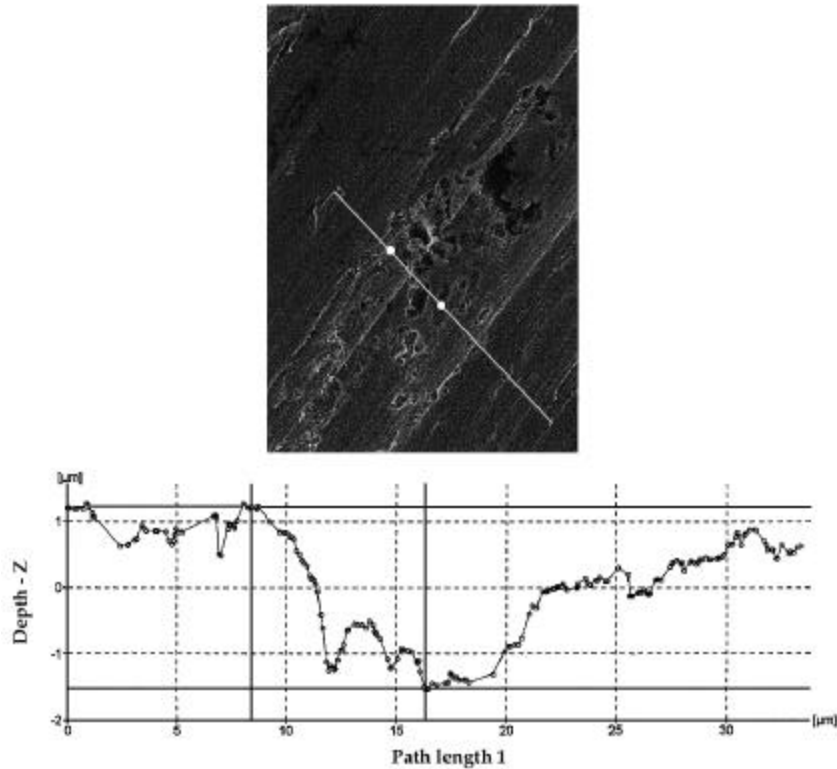


**Fig. 4. Representative profile analysis for the virgin coupon surface.** Relative elevation along the trace (white line in photo) is given by the graph at the bottom. In this case, the elevation difference between the high point and low point (large dots on trace) is about 1  $\mu\text{m}$ . Except for isolated areas (from which inclusions have been pulled to create a pit-like region), the bulk surface is smooth with nominal surface relief approximately 0.5 $\mu\text{m}$ .

In contrast to the unexposed coupon, the surface of the specimen exposed to mercury under cavitation conditions exhibits much more surface relief over essentially the entire coupon surface. Figure 5 gives representative examples of this observation, and the coupon surface appears to exhibit a “corroded” surface. The profile analysis in Fig. 6 indicates a generally rougher surface with many “pits” approximately 14  $\mu\text{m}$  deep.

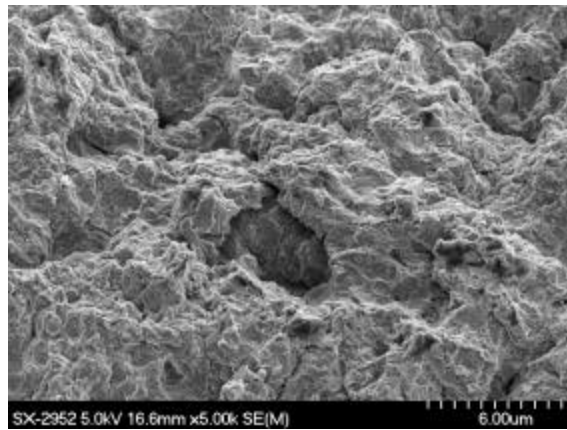
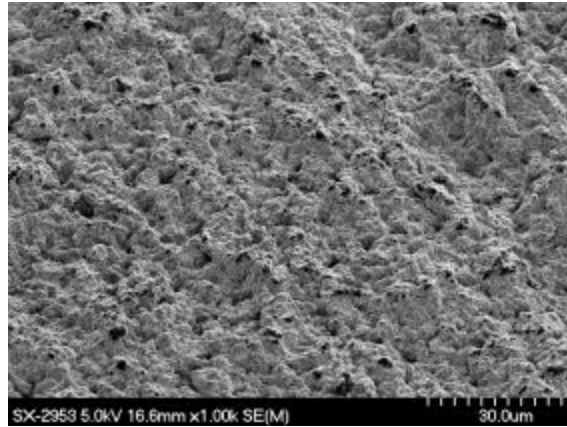


**Fig. 5. Scanning electron microscope images of the surface of the 316L coupon exposed to cavitation conditions in mercury.** Compared to the virgin coupon shown in Fig. 3, the surface here is rough and irregular.

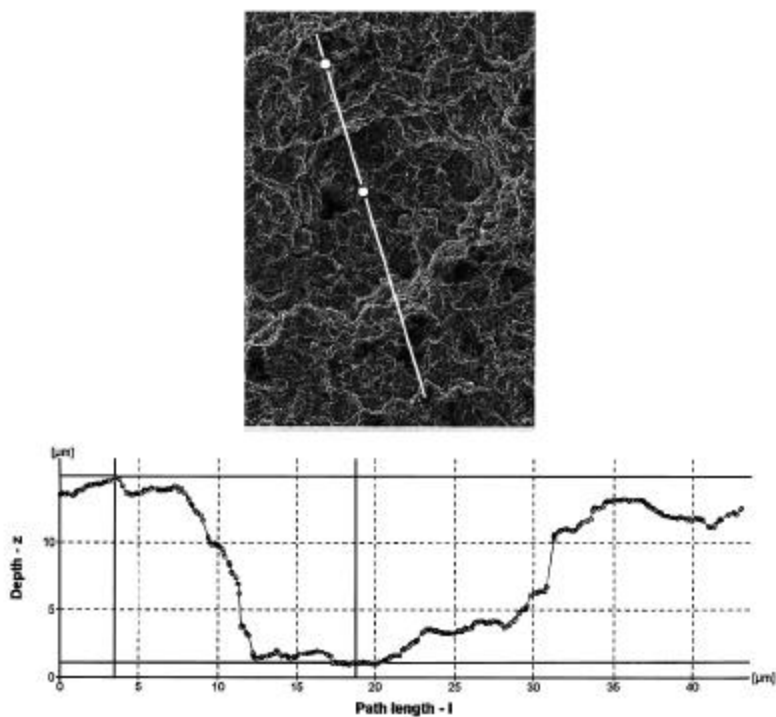


**Fig. 6. Representative profile analysis for a 316L coupon exposed to cavitation conditions in the bench-top experiment.** Relative elevation along the trace (white line in photo) is given by the graph at the bottom. In this representative case, the elevation difference between the high point and low point (large dots on trace) is almost 15  $\mu\text{m}$ . Even deeper “pits” are evident in this area.

Electron microprobe chemical analysis of the surface and cross section of the specimen exposed to room temperature cavitation in mercury did not reveal any leaching of chromium or nickel (which was observed in the case of the maximum interaction of 316L with mercury).<sup>6</sup> It is possible that the initial development of a very thin layer depleted in nickel and/or chromium coincides with its mechanical removal from the surface due to erosion, as any leaching reaction renders the affected material structurally weakened and more susceptible to erosion. However, it is also likely that the low temperature ambient exposure was inadequate to leach significant nickel and chromium even if chemical wetting had been established.

Immediately following exposure to the mercury under cavitation conditions, mercury appeared to cling to large areas of surface suggesting some amount of “wetting.” However, the

mercury was easily removed from the surface for post-test analysis and, with the exception of a very few small, isolated beads resting in the surface relief, no mercury was found on the post-test surface after cleaning.

Taken together, these observations suggest that the exposure of the coupon to room temperature cavitation contributes to significant mechanical damage to the surface (akin to erosion), but it is not clear if this is accompanied by chemical interaction with the mercury. However, the physical removal of material from the coupon surface as a result of cavitation under these conditions suggests a possible damage mechanism in the SNS target. Cavitation also appears to be a means to develop chemical wetting in the standard TCL by removal of the passive film from 316L while immersed in mercury.

Further evaluation of the cavitation issue was undertaken using a cylindrical 316L stainless steel tube section of the same diameter as that used in fabrication of the TCLs (rather than a glass tube). Several combinations of coupon placement in the tube, e.g., centered, off-center, and at various depths, and waveform/frequency combinations were evaluated to confirm a visual appearance of wetting/interaction for coupons exposed to room temperature cavitation in mercury. Based on these results, it was deemed appropriate to modify the standard TCL design by adding an ultrasonic transducer to generate cavitation.



### 3. MODIFIED TCL EXPERIMENTS

Following the proof-of-concept tests, the standard TCL design was modified to include an ultrasonic transducer near the top of the hot leg, which is the heated vertical length of tubing in which the highest TCL temperatures are generated. Details of the standard loop design and construction are recorded elsewhere,<sup>6-8</sup> and Fig. 7 shows the schematic TCL design with modifications made for this experiment.

An approximately 8-cm length of TCL tubing was cut from the region just below the thermocouple well at the top of the hot leg. In its place, a section of tubing from the same heat of material with a donut-shaped transducer affixed with high temperature epoxy was welded as shown in Fig. 7. In addition, a standard flange was welded to the top of the hot leg opening to facilitate placement of the specimens into the area receiving ultrasonic energy.

Rather than using an interlocked chain of rectangular 316L coupons as in previous TCL tests,<sup>6-8</sup> small pieces of tubing were placed in a stack on a welding wire mounted in the top of the hot leg via a flange. The tubing from which the specimens were cut was mill-annealed 316L with an OD of 3.2 mm and an ID of 2.0 mm, and each specimen was 6.0 mm in length. The welding wire on which the cylindrical specimens were stacked was approximately 1.7 mm in diameter. The individual specimens in the stack were numbered and then cleaned ultrasonically in acetone prior to loading in the stack. The individual specimens were placed such that they were centered at the vertical location of the transducer, as shown in Fig. 7, allowing several individual specimens to be placed 2-3 cm above and below the precise position of the transducer as well as adjacent to the transducer. The remaining space on the specimen stack was filled with long pieces of the same 3.2 mm tubing; with the bottom end held firmly in place by a tubing-to-wire spot weld. This specimen arrangement was found to hold the specimens rigidly in place during each test and to permit easy disassembly of the specimen stack for evaluation and reassembly for the next test.

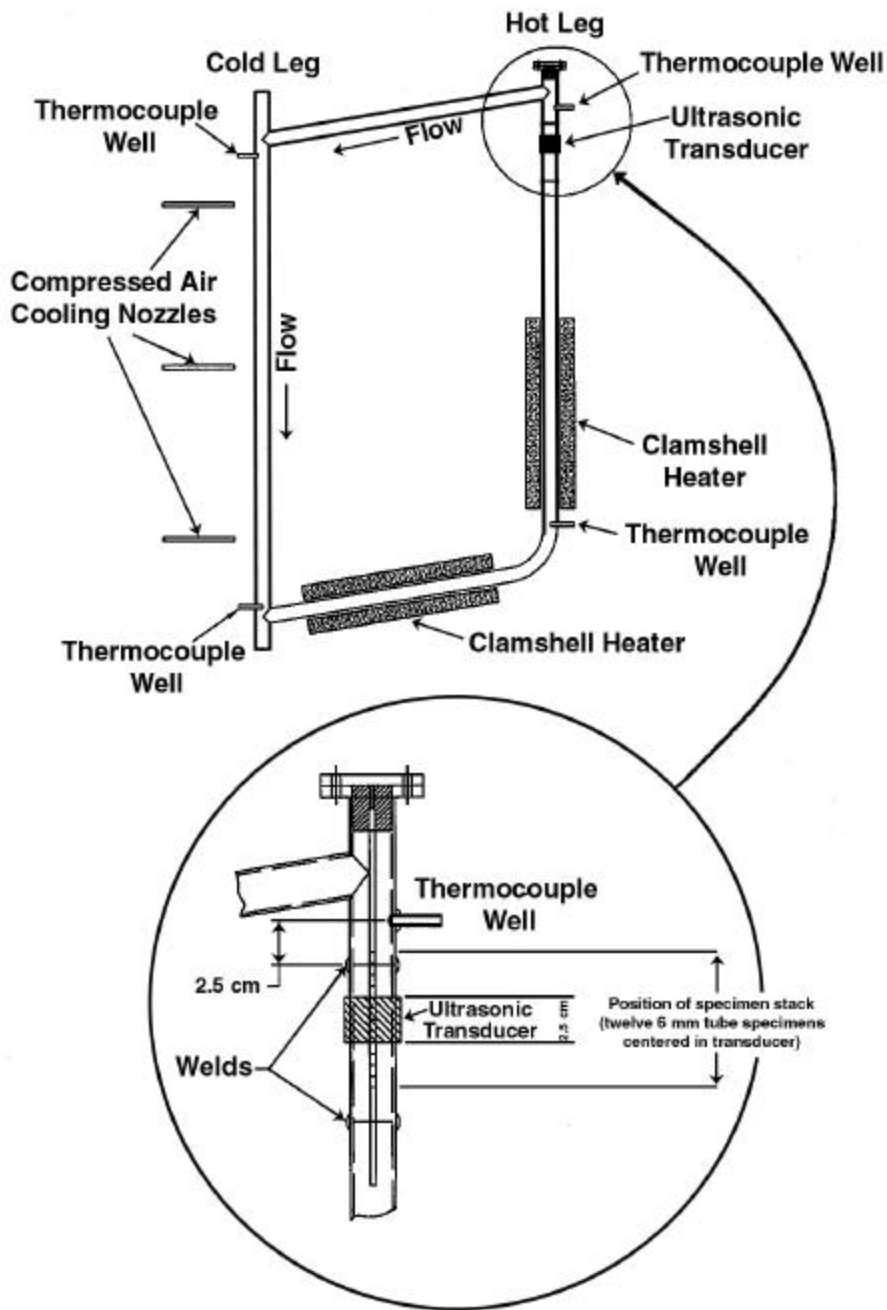


**Fig. 7. Schematic diagram of TCL modified by the addition of an ultrasonic transducer.** Overall, the actual loop is about 1 m in height and about half that wide. The tubing is 316L stainless steel of 2.5 cm diameter.

The experimental plan called for a series of 48-72 h test exposures to determine the optimum conditions for operating the transducer to develop appropriate – and reproducible –



cavitation and interaction with the specimen surfaces. Once these conditions were determined for the assembled TCL, a set of virgin specimens would be placed on the stack and operation of the TCL initiated. The plan called for operating the TCL with the same overall temperature gradient as in previous tests<sup>6-8</sup> to generate a similar natural convection flow rate, except that the overall temperature would be lower (maximum 130°C, minimum 70°C) to more accurately represent SNS conditions and to prevent destroying the transducer. After 48-72 h of operation with the transducer energized, power to the transducer would be stopped and the TCL operated at the reduced temperature for an extended time. Posttest analysis would reveal if the mechanical damage to the specimens during the initial portion of the test “encouraged” interaction of mercury with the specimens that previously were not observed at such low exposure temperatures.

The initial TCL test was performed for transducer settings determined to produce cavitation on the rectangular coupons in the small section of loop tubing in the previous bench-top tests, which included a frequency of 27.5 kHz with the wave form generator power supply at 10 v peak-to-peak. The frequency setting was occasionally adjusted ( $\pm 0.2$  kHz) to maximize the audible noise coming from the TCL, which was indicative of cavitation bubbles in the region of the transducer. The frequency was maintained in the range 27.1–27.5 kHz for 48 h, with occasional checks of the peak-to-peak voltage observed on the oscilloscope and audible noise from the loop as feedback that cavitation was occurring somewhere inside the loop. A thermocouple externally mounted on the TCL wall adjacent to the transducer indicated  $<1^{\circ}\text{C}$  temperature rise at that location during the experiment. Following this exposure, none of the removable specimens revealed any change in appearance (still smooth and shiny, no clinging mercury) or any weight change.

The specimen stack was reassembled and another TCL cavitation experiment attempted. In this case, the driver frequency was doubled to 54.2 kHz with the power supply setting remaining at 10 volts peak-to-peak. However, after the first few hours at this setting, the audible

feedback from the loop ceased and minor adjustments to the frequency could not re-establish the prior noise level, indicating that cavitation had ceased. The frequency was subsequently adjusted to 36.5 kHz, at which value the noise from internal cavitation resumed, and with only minor adjustment, the test completed 48 additional hours at this frequency with no rise in local temperature. Again, however, post-test examination revealed no change in appearance or weight for any of the coupons.

The third TCL experiment utilized a frequency of 42.2 kHz with a power supply setting of 6.2 v. With only minor frequency adjustments, this experiment accumulated 60 h with no rise in local temperature. Again, however, post-test examination revealed no discernable change in any of the coupons.

At this point, the TCL was partially drained of mercury such that a bore scope could be inserted into the hot leg to (and past) the position of the transducer to look for cavitation damage on surfaces other than the removable specimens. The ID surfaces of the TCL tubing were examined over a range of several cm above and below the position of the transducer and found to be bright and shiny, and very smooth – only a few scattered drawing marks from the original fabrication of the tube were observed. This result indicates that the cumulative “damage” for the three tests in the TCL, which included more than six days at various conditions, left no readily apparent sign of cavitation or wetting on the TCL surfaces. The only minor sign of wetting (clinging mercury) was observed on the thermocouple well at the top of the hot leg. This piece of 316L tubing - but not the TCL walls adjacent to the tubing - appeared “silvered” by a thin film of mercury. This result suggests that the pressure wave energy was inadvertently focused away from the specimens and that, perhaps, the thermocouple well was acting as the initiator for cavitation onset. This result could not have been predicted from the simplified bench-top experiments, in which only a short cylinder was used compared to the complex geometry of a TCL.

Inability to reproduce cavitation damage in the TCL of the type generated in the bench-top tests in glass and stainless steel tubing led to the discontinuation of these experiments prior to the planned long-term exposure. It is not clear why cavitation/wetting could not be reproduced in the TCL. In addition to the thermocouple well acting as an initiator as noted above, it is possible the small volume in the bench-top vessel confined the acoustic energy in a way that made it more focused and destructive compared to the very large mercury volume and essentially “infinite” test cylinder of the hot leg in the TCL. In addition, the shape of the test specimens (cylindrical in the TCL and flat rectangles in the bench-top tests) and/or the protuberances inside the TCL perhaps contributed to a geometry effect, which was not anticipated from the simplified bench-top tests. In any case, the attempt to use acoustic energy to generate cavitation and aid wetting in the TCL was considered unsuccessful for practical use.



#### **4. CONCLUSIONS**

Bench-top experiments exposing 316L coupons to cavitation conditions with acoustic pressure waves of frequency 20 kHz and 1.5 MPa amplitude resulted in apparent wetting by mercury at room temperature as well as substantial erosion-like wastage in only 24 h. Attempts to use the cavitation mechanism to generate relatively low temperature wetting in a thermal convection loop proved unsuccessful, due perhaps to geometrical differences/relationships between the internals of the TCL and the bench-top experiments. Wetting remains a somewhat enigmatic phenomenon for stainless steel surfaces in mercury.



## **ACKNOWLEDGMENTS**

The authors would like to acknowledge the helpful role of many individuals. H. F. Longmire performed the specimen metallography, and L. R. Walker provided the scanning electron microscopy and microprobe analysis. R. B. Ogle and S. N. Lewis provided Industrial Hygiene advice and services for controlling mercury exposures. Throughout this research effort, J. H. DeVan (recently deceased) provided many helpful discussions and insights, and he will be sorely missed. P. F. Tortorelli and L. K. Mansur provided critical review of the manuscript. F. C. Stooksbury and K. A. Choudhury and helped prepare the manuscript and figures.





## REFERENCES

1. L. K. Mansur and H. Ullmaier, compiled *Proceedings of the International Workshop on Spallation Materials Technology*, CONF-9604151, Oak Ridge, TN, April 23-25, 1996.
2. L. F. Epstein, in *Liquid Metals Technology – Part I*, F. J. Antwerpen, ed. “Static and Dynamic Corrosion and Mass Transfer in Liquid Metal Systems,” *Chemical Engineering Progress Symposium Series*, 53(20), p.67, 1957.
3. J. R. DiStefano, *A Review of the Compatibility of Containment Materials with Potential Liquid Metal Targets*, ORNL/TM-13056, August 1995.
4. J. R. Weeks, “Liquidus Curves and Corrosion of Fe, Cr, Ni, Co, V, Cb, Ta, Ti, and Zr in 500-750°C Mercury,” *Corrosion* 23(4), p.98, 1967.
5. J. R. DiStefano, S. J. Pawel, and E. T. Manneschildt, *Materials Compatibility Studies for the Spallation Neutron Source*, ORNL/TM-13675, September 1998.
6. S. J. Pawel, J. R. DiStefano, and E. T. Manneschildt, *Corrosion of Type 316L Stainless Steel in a Mercury Thermal Convection Loop*, ORNL/TM-13754, April 1999.
7. S. J. Pawel, J. R. DiStefano, and E. T. Manneschildt, *Effect of Surface Condition and Heat Treatment on Corrosion of Type 316L Stainless Steel in a Mercury Thermal Convection Loop*, ORNL/TM-2000/195, July 2000.
8. S. J. Pawel, J. R. DiStefano, and E. T. Manneschildt, *Effect of Mercury Velocity on Corrosion of Type 316L Stainless Steel in a Thermal Convection Loop*, ORNL/TM-2001/18, February 2001.
9. R. P. Taleyarkhan, et. al., “Experimental Determination of Cavitation Thresholds in Liquid Water and Mercury,” *Proceedings of the 2<sup>nd</sup> International Topical Meeting on Nuclear Applications of Accelerator Technology (AccApp98)*, Gatlinburg, TN, September 1998.
10. F. Moraga and R. P. Taleyarkhan, *Static and Transient Cavitation Threshold Measurements in Mercury*, *Proceedings of the 3<sup>rd</sup> International Topical Meeting on Accelerator Applications (AccApp99)*, Long Beach, CA, November 1999.
11. R. P. Taleyarkhan, et. al., “Thermal Shock Assessments for the SNS Target System,” *Proceedings of the International Topical Meeting on Advanced Reactor Safety (ARS’97)*, Orlando, FL, June 1997.
12. M. D. Kass, et. al., *Tribology Letters* 5 (1998) 231-234.



## Internal Distribution

1. R. R. Allen
2. R. E. Battle
3. E. E. Bloom
4. K. K. Chipley
5. J. E. Cleaves
6. J. W. Cobb
7. H. H. Cromwell
8. J. R. DiStefano
9. D. A. Everitt
10. K. Farrell
11. T. A. Gabriel
12. J. R. Haines
13. L. L. Horton
14. J. D. Hunn
15. L. L. Jacobs
16. D. R. Johnson
17. J. O Johnson
- 18-22. S. H. Kim (5)
23. R. D. Lawson
24. D. C. Lousteau
25. A. T. Lucas
26. E. T. Manneschmidt
27. L. K. Mansur
28. T. E. Mason
29. T. J. McManamy
30. G. E. Michaels
31. A. E. Pasto
- 32-36. S. J. Pawel (5)
37. M. J. Rennich
38. S. L. Schrock
39. P. T. Spampinato
40. C. H. Strawbridge
41. J. P. Strizak
- 42-46. R. P. Taleyarkhan (5)
47. P. F. Tortorelli
48. J. H. Whealton
49. D. K. Wilfert
50. G. L. Yoder
- 51-52. Central Research Library (2)
53. Document Reference Section
- 54-55. ORNL Laboratory Records – RC (2)
56. Office of Scientific and Technical

## External Distribution

57. G. Bauer, Paul Scherrer Institute, CH-5232, Villigen-PSI, Switzerland
58. J. M. Carpenter, Argonne national Laboratory, 9700 south Cass Avenue, Building 360, IPNS Division, Argonne, IL 60439
59. A. Jason, Los Alamos National Laboratory, P. O. Box 1663, H817 LANSCE-1, Los Alamos, NM 87545
60. P. Liaw, University of Tennessee, Department of Materials Science 7 Engineering, 427-B Doutherty Building, Knoxville, TN 37996-2200
61. W. Sommer, Los Alamos national Laboratory, P. O. Box 1663, LANSCE-2, Los Alamos, NM 87545
62. M. Todosow, Brookhaven National Laboratory, P. O. Box 5000, Building 475B, Upton, NY 11973
63. M. Wechsler, 106 Hunter Hill Place, Chapel hill, NC 27514-9128
64. W. Wang, Brookhaven National Laboratory, P. O. Box 5000, Building 911B, Upton, NY 11973

